



## The anti-perovskite type hydride $\text{InPd}_3\text{H}_{0.89}$

H. Kohlmann<sup>a,\*</sup>, A.V. Skripov<sup>b</sup>, A.V. Soloninin<sup>b</sup>, T.J. Udovic<sup>c</sup>

<sup>a</sup> Universität des Saarlandes, Fachrichtung 8.1—Anorganische Festkörperchemie, Am Markt, Zeile 3, 66125 Saarbrücken, Germany

<sup>b</sup> Institute of Metal Physics, Urals Branch of the Russian Academy of Sciences, S. Kovalevskoi 18, Ekaterinburg 620041, Russia

<sup>c</sup> NIST Center for Neutron Research, National Institute of Standards and Technology, 100 Bureau Drive, Gaithersburg, MD 20899-6102, USA

### ARTICLE INFO

#### Article history:

Received 24 June 2010

Accepted 8 August 2010

Available online 12 August 2010

#### Keywords:

Metal hydrides

Palladium

Neutron powder diffraction

Inelastic neutron scattering

Nuclear magnetic resonance spectroscopy

### ABSTRACT

Hydrogenation of tetragonal  $\text{InPd}_3$  in the  $\text{ZrAl}_3$  type structure (four-fold ccp superstructure) yields a hydride with a cubic  $\text{AuCu}_3$  type structure (one-fold ccp superstructure). Deuterium can be located by neutron powder diffraction in octahedral voids surrounded exclusively by palladium,  $[\text{Pd}_6]$ , which are 88.5(6)% occupied in a statistical manner. The resulting deuteride  $\text{InPd}_3\text{D}_{0.89}$  thus crystallizes in a cubic anti-perovskite type structure (space group  $Pm\bar{3}m$  (no. 221),  $a=402.25(1)$  pm at 299(2) K). The Pd–D distance of 201.13(1) pm is typical for interstitial hydrides with palladium. Inelastic neutron scattering on the hydride  $\text{InPd}_3\text{H}_{0.89}$ , which shows a spectrum similar to that of binary palladium hydride, confirms the cubic site symmetry of hydrogen in  $[\text{Pd}_6]$  interstices. This is also confirmed by the absence of any quadrupole splitting in the  $^2\text{D}$ -NMR signal of the deuteride.  $^1\text{H}$  NMR spectra of  $\text{InPd}_3\text{H}_{0.89}$  do not show any motional narrowing. Values found for the H jump rate  $\tau^{-1}$  in  $\text{InPd}_3\text{H}_{0.89}$  remain below  $10^6 \text{ s}^{-1}$  in the studied temperature range 28–360 K, indicating a small hydrogen mobility in  $\text{InPd}_3\text{H}_{0.8}$  as compared with binary palladium hydride,  $\text{PdH}_{\leq 1}$ . This can be attributed to the large spatial separation of the  $[\text{Pd}_6]$  sites.

© 2010 Elsevier Inc. All rights reserved.

### 1. Introduction

It has long been known since the 19th century [1,2] that palladium can take up considerable amounts of gaseous hydrogen. Ever since, palladium and palladium containing intermetallic phases have been used as model systems to ascertain the effect of hydrogen uptake on the structural, magnetic, electronic, optical, and mechanical properties of metallic systems [3–5]. Crystal structures and bonding properties of the ternary palladium hydrides show a huge variation, from the metallic interstitial hydrides, which can possess a variable hydrogen content [5], to the semiconducting complex hydrides with covalent palladium–hydrogen bonding involving 18-electron anionic hydrido metalate complexes with fixed hydrogen content [6,7].

Crystal structures of Pd-rich intermetallics often resemble that of the cubic close packing (ccp, Cu type) of palladium itself. In the case of main-group metals substituting for palladium, ordered superstructures are typically found instead of ccp-based solid solutions. For some of these Pd-rich intermetallic compounds forming ccp superstructures, H-induced rearrangement of the atoms was observed. In  $\text{MnPd}_3$  [8],  $\text{MgPd}_3$  [9], and  $\text{TlPd}_3$  [10], the metal sublattice changes from a tetragonal four-fold ccp superstructure ( $\text{ZrAl}_3$  type with  $a, a, 4a$ ) to a cubic  $\text{AuCu}_3$  type with

hydrogen (deuterium) incorporated into  $[\text{Pd}_6]$  voids surrounded exclusively by palladium atoms. X-ray powder diffraction and *in situ* thermal analysis data indicate that the same type of transformation also occurs in  $\text{InPd}_3$  starting from either its  $\text{ZrAl}_3$  or  $\text{TiAl}_3$  type structural arrangement [11]. Hydrogen (deuterium) positions in the hydride (deuteride) formed have thus far not been determined. In this paper, we report on the full crystal structure of the deuteride of  $\text{InPd}_3$  and the location of deuterium atoms by neutron powder diffraction (NPD), as well as on the dynamics of hydrogen by inelastic neutron scattering (INS) and nuclear magnetic resonance (NMR) spectroscopy.

### 2. Experimental details

#### 2.1. Synthesis of intermetallic compounds, hydrides, and deuterides

Stoichiometric mixtures of indium pieces (99.99%, Schuchardt<sup>1</sup>) and palladium powder (99.9%, < 60  $\mu\text{m}$ , ChemPur) were placed in a silica tube and 0.35 mol% (with respect to In) of freshly sublimed iodine added to enhance the reactivity by means of chemical vapor transport. The silica ampoules were heated 50 K/h to 850 K,

<sup>1</sup> Certain commercial suppliers are identified in this paper to foster understanding. Such identification does not imply our recommendation or endorsement nor does it imply that the materials or equipment identified are necessarily the best for the purpose.

\* Corresponding author.

E-mail address: [h.kohlmann@mx.uni-saarland.de](mailto:h.kohlmann@mx.uni-saarland.de) (H. Kohlmann).

held at this temperature for 56 h, and quenched in air. Iodine was sublimed off the products by gently heating one end of the sealed silica tube. This procedure yields  $\text{InPd}_3$  in the tetragonal  $\text{ZrAl}_3$  type [12] as a gray powder. Finely ground  $\text{InPd}_3$  powder was put in crucibles machined from hydrogen-resistant Nicrofer(R) 5219 Nb-alloy718 and charged with hydrogen (7.0 MPa for the hydride of  $\text{InPd}_3$  used for INS and NMR; 99.999%, Praxair) or deuterium gas (4.5 MPa for the deuteride used for NPD and NMR; isotopic purity 99.8%, chemical purity 99.999%, Praxair) in an autoclave made from the same alloy. The autoclave was heated within 2 h to 500 K for the hydride and 523 K for the deuteride and held at those temperatures for 46 h for the hydride and for 24 h for the deuteride. After cooling back to room temperature, the gas pressure was released. None of the hydrogenated (deuterated) samples was found to be sensitive to air.

## 2.2. X-ray powder diffraction (XRPD)

XRPD data were collected using flat transmission samples containing an internal silicon standard on an image plate Guinier powder diffractometer (Huber Guinier camera G670 at  $T=296(1)$  K with  $\text{Cu K}\alpha_1$  radiation,  $\lambda=154.056$  pm). Rietveld refinements were carried out with the program FULLPROF [13] and pseudo-Voigt as the profile function.

## 2.3. Neutron powder diffraction (NPD)

Neutron powder diffraction data on deuterated  $\text{InPd}_3$  were taken at  $T=299(2)$  K on the high resolution powder diffractometer D1A at the Institute Laue-Langevin in Grenoble, France, in the range  $6^\circ \leq 2\theta \leq 157^\circ$  (step size  $\Delta 2\theta=0.05^\circ$ ) during a total measuring time of 12 h. Special care was taken for the enhanced neutron absorption of indium by using a moderate sample thickness (3.2 g  $\text{InPd}_3$  powder in a vanadium can of 5 mm inner diameter, sealed by indium wire). The wavelength used was determined from a measurement on a silicon standard to be  $\lambda=190.931(3)$  pm for D1A and kept fixed during refinements.

## 2.4. Inelastic neutron scattering (INS)

Inelastic neutron scattering measurements of the hydrogen vibrational spectrum at 4 K were performed on the filter-analyzer neutron spectrometer (FANS) [14] at the NIST Center for Neutron Research (Gaithersburg, MD, USA). The measured range of the neutron energy loss was 40–208 meV with an energy resolution varying from 2.4% to 3.3% of the energy transfer.

## 2.5. Nuclear magnetic resonance spectroscopy (NMR)

NMR measurements were performed on a modernized Bruker SXP pulse spectrometer with quadrature phase detection at the frequencies  $\omega/2\pi=23.8$  and 90 MHz (for  $^1\text{H}$ ) and 61.4 MHz (for  $^2\text{D}$ ). For  $^1\text{H}$  NMR measurements, the magnetic field was provided by a 2.1 T iron-core Bruker magnet, and a home-built multi-nuclear continuous-wave NMR magnetometer working in the range 0.32–2.15 T was used for field stabilization. For  $^2\text{D}$  NMR measurements, the magnetic field was provided by a 9.4 T Oxford superconducting solenoid. For rf pulse generation, we used a home-built computer-controlled pulse programmer, the PTS frequency synthesizer (Programmed Test Sources, Inc.), and a 1 kW Kalmus wideband pulse amplifier. Typical values of the  $\pi/2$  pulse length were 2–3  $\mu\text{s}$ . A probehead with the sample was placed into an Oxford Instruments CF1200 continuous-flow cryostat using helium or nitrogen as cooling agents. The sample temperature, monitored by a chromel-(Au-Fe) thermocouple, was

stable to  $\pm 0.1$  K. The nuclear spin-lattice relaxation rates were measured using the saturation–recovery method. In all cases, the recovery of the nuclear magnetization could be satisfactorily described by a single exponential function. NMR spectra were recorded by Fourier transforming the spin echo signals.

## 3. Results and discussion

### 3.1. The crystal structure of $\text{InPd}_3\text{H}_{0.89}$

$\text{InPd}_3$  was shown to belong to a group of compounds  $\text{MPd}_3$  with tetragonal superstructures of the cubic close packing (ccp), which exhibit a considerable reactivity towards hydrogen and form binary hydrides  $\text{MPd}_3\text{H}_{\leq 1}$ . Upon hydrogenation (deuteration),  $\text{InPd}_3$  transforms from either a tetragonal  $\text{TiAl}_3$  (two-fold ccp superstructure) or a tetragonal  $\text{ZrAl}_3$  type arrangement (four-fold ccp superstructure) to a cubic  $\text{AuCu}_3$  type (one-fold ccp superstructure,  $a=402.702(4)$  pm for the hydride,  $a=402.25(1)$  pm for the deuteride at  $T=299(2)$  K) for the metal sublattice as shown by XRPD [11]. Neutron powder diffraction (NPD) experiments on a deuterated sample of  $\text{InPd}_3$  now confirm this finding. Fig. 1 shows the NPD data that are in accordance with a single phase of cubic  $\text{InPd}_3$  ( $\text{AuCu}_3$  type) with interstitial deuterium atoms. The location of deuterium positions was found by difference Fourier techniques. Deuterium was found to occupy octahedral interstices surrounded by palladium atoms only,  $[\text{Pd}_6]$ , with an occupation of 88.5(6)% in a statistical manner, while other octahedral voids like  $[\text{In}_2\text{Pd}_4]$  are empty. Full occupation of this site would correspond to a cubic perovskite type  $\text{AMX}_3$ , in which the metal M occupies the position of the non-metal X and vice versa. The resulting  $\text{AXM}_3$  type is often called cubic anti-perovskite, although not all cation and anion positions are interchanged. Thus, the structure of the hydride (deuteride) of  $\text{InPd}_3$  can be considered as a defect variant of the cubic anti-perovskite type (Table 1, Fig. 2) and the refined deuterium content corresponds to the formula  $\text{InPd}_3\text{D}_{0.89}$ .

The palladium–deuterium distance of 201.13(1) pm is comparable to the palladium–deuterium distances in the isotopic  $\text{MnPd}_3\text{H}_{0.7}$  (196.3 pm [15]) and  $\beta\text{-MgPd}_3\text{H}_{0.7}$  (199.10(1) pm [9]), but is considerably longer than in typical homoleptic hydrido palladium complexes (160–184 pm [16]), indicating a metallic rather than a covalent metal–deuterium bonding. This agrees well with the dynamic behavior of hydrogen typical for metallic hydrides (see Section 3.2). In contrast to the cubic anti-perovskite type deuteride  $\text{CeRh}_3\text{D}_{0.84}$  [17], the deuterium atom in  $\text{InPd}_3\text{D}_{0.89}$

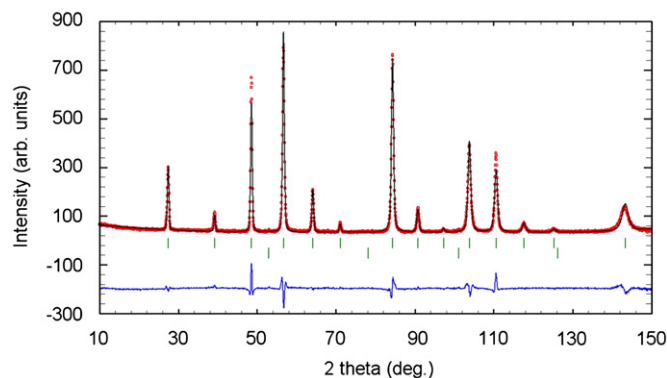
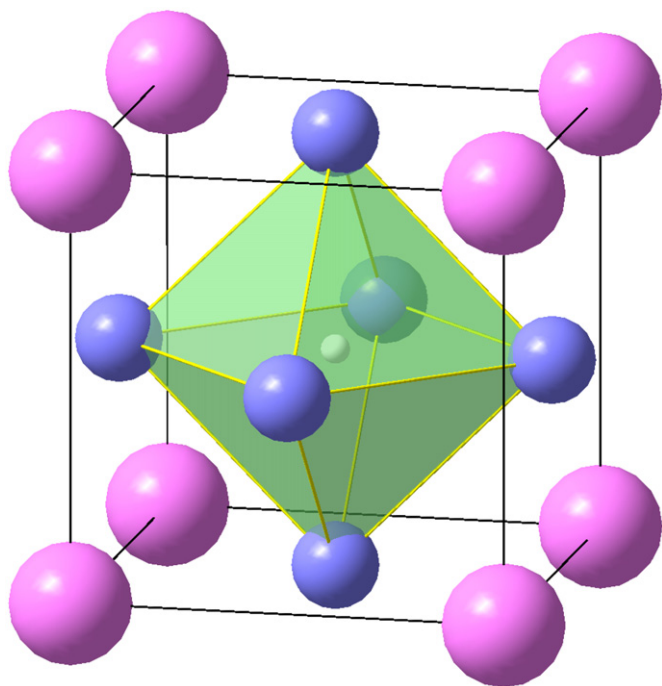


Fig. 1. Rietveld refinement of the crystal structure of  $\text{InPd}_3\text{D}_{0.89}$  from neutron powder diffraction data (D1A at ILL (Grenoble, France),  $\lambda=190.931(3)$  pm,  $T=299(2)$  K). Observed (circles), calculated (solid line), and difference (observed–calculated; bottom) neutron powder diffraction patterns. Markers indicate Bragg peak positions of  $\text{InPd}_3\text{D}_{0.89}$  (top) and V from the sample holder (bottom).

**Table 1**Crystal structure data of  $\text{InPd}_3\text{D}_{0.89}$  as refined from neutron powder diffraction data at room temperature ( $T=299(2)$  K) and interatomic distances (pm) below 350 pm.

Space group $Pm\bar{3}m$ (no. 221), $a=402.25(1)$ pm, $Z=1$							
Atom	Site	x	y	z	$B_{\text{iso}}/10^4 \text{ pm}^2$	Occupation	
In	1a	0	0	0	0.11(5)	1	
Pd	3c	0	1/2	1/2	0.36(3)	1	
D	1b	1/2	1/2	1/2	1.66(7)	0.885(6)	
$R_p=0.060$	$R_{wp}=0.075$	$R'_p=0.281$	$R'_{wp}=0.138$	$R_{\text{Bragg}}=0.030$	$S=2.26$		
Pd—2D	201.13(1)	In—8D	348.36(1)	D—6Pd	201.13(1)		
Pd—4In	284.43(1)	In—12Pd	284.43(1)	D—8In	348.36(1)		
Pd—8Pd	284.43(1)						

Definition of  $R$  factors:  $R_p = \sum |y_i(\text{obs}) - y_i(\text{calc})| / \sum y_i(\text{obs})$ ;  $R_{wp} = [\sum w_i (y_i(\text{obs}) - y_i(\text{calc}))^2 / \sum w_i y_i(\text{obs})^2]^{1/2}$ ;  $R'_p$  and  $R'_{wp}$  are calculated as above but using background corrected counts;  $R_{\text{Bragg}} = \sum |I_B(\text{obs}') - I_B(\text{calc})| / \sum I_B(\text{obs}')$ . Form of the temperature factor:  $\exp[-B_{\text{iso}}(\sin \theta/\lambda)^2]$ .



**Fig. 2.** Crystal structure of  $\text{InPd}_3\text{D}_{0.89}$  in the cubic anti-perovskite type (In: large, pink spheres; Pd: middle, blue; D: small, white) (for interpretation of the references to color in this figure legend, the reader is referred to the web version of this article).

exhibits a rather moderate thermal displacement parameter, which may be explained by the smaller  $[\text{Pd}_6]$  void in the latter as compared to the former. As in other hydrides, e.g.  $\text{LaNiInD}_{1.63}$  [18] or  $\text{Ba}_9\text{In}_4\text{H}$  [19], hydrogen (deuterium) does not coordinate indium. In  $\text{InPd}_3\text{D}_{0.89}$ , deuterium atoms avoid the neighborhood of indium by occupying only  $[\text{Pd}_6]$  voids.

Hydrides of intermetallics with non-stoichiometric composition with respect to hydrogen often exhibit temperature driven ordering phenomena within the hydrogen substructure, giving rise to structural phase transition and drastic changes in hydrogen diffusion properties [20,21]. However, since the large spatial separation of these deuterium sites in  $\text{InPd}_3\text{D}_{0.89}$  (shortest distance is  $a=402.25(1)$  pm) is well above the so-called 'blocking radius' [20], the D–D repulsion is relatively low, making ordering at low temperatures less likely. Nonetheless, whether or not ordering occurs in such  $\text{MPd}_3$  hydrides (deuterides) is an open question, regarding which the INS and NMR measurements reported in the next section may shed some light. These were also performed with the aim to learn more about possible diffusion

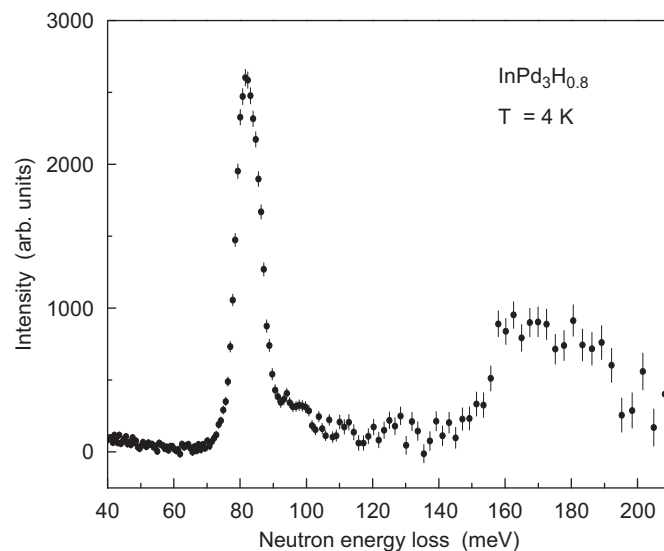


**Fig. 3.** The low-temperature INS spectrum for  $\text{InPd}_3\text{H}_{0.89}$ . Vertical error bars associated with the data points correspond to one standard deviation.

processes. Contrary to many other intermetallic hydrides, the hydrogen positions in  $\text{MPd}_3$  ( $M=\text{Mg, In, Tl, Mn}$ ) are well separated from each other, i.e., long-range hydrogen diffusion pathways would have to involve  $[\text{M}_2\text{Pd}_4]$  voids, which thus far were only found to be occupied in the  $\alpha$  modification of the hydride  $\text{MgPd}_3\text{H}_{0.79 \leq x \leq 0.94}$  [22]. Despite the structural similarities to  $\text{PdH}_x$  (i.e., the same hydrogen local environment) in which hydrogen exhibits rather fast diffusion processes, there is no direct information on hydrogen diffusion rates in  $\text{MPd}_3$  hydrides.

### 3.2. Hydrogen dynamics in $\text{InPd}_3\text{H}_{0.89}$

For metal-hydrogen systems, inelastic neutron scattering (INS) spectra in the energy transfer range 40–150 meV are usually dominated by the fundamental modes of H optical vibrations. The simplest description of these vibrations is based on the model of a three-dimensional Einstein oscillator [23,24]. For the cubic point symmetry of H sites, this model predicts a single peak in an INS spectrum in the energy transfer range of the fundamental modes. For lower point symmetries of H sites, this peak should be split into either two peaks with the intensity ratio 2:1 (for axial symmetry) or three peaks of nearly equal intensity (for symmetries lower than axial). The measured low-temperature INS spectrum for  $\text{InPd}_3\text{H}_{0.89}$  is shown in Fig. 3. This spectrum is dominated by a single peak

centered at the energy transfer of 82 meV. This is consistent with the neutron diffraction data showing that H atoms occupy only the octahedral sites with  $[Pd_6]$  coordination. If a considerable fraction of H atoms were located at the sites with  $[In_2Pd_4]$  coordination, we would expect a splitting of the sharp peak of the INS spectrum. The small high-energy ‘shoulder’ near 100 meV is almost certainly an optoacoustic multiphonon sideband originating from a combination of the fundamental optical mode and the lower-energy acoustic phonon band, as typically seen in other metal-hydride systems [25,26]. The broad band centered at the energy transfer of  $\sim 175$  meV can be attributed to the second-order (two-phonon) transition, which is expected to appear at nearly double the energy of the fundamental peak.

The shape of the INS spectrum for  $InPd_3H_{0.89}$  resembles but is considerably sharper than that for  $PdH_x$  [24,27,28]. This is not surprising since, in  $PdH_x$ , hydrogen atoms also occupy the octahedral interstitial sites coordinated by six Pd atoms. However, for  $PdH_x$ , the main peak is centered at lower values of the energy transfer (56–69 meV, depending on the H concentration [24]), reflecting a somewhat weaker bonding potential. Moreover,  $PdH_x$  exhibits a much more pronounced high-energy ‘shoulder’ originating from longitudinal optic modes with strong dispersion due to significant H–H interactions [29] with the much smaller optoacoustic multiphonon sideband buried underneath. In contrast to  $PdH_x$ , no neighboring octahedral sites are occupied in  $InPd_3H_{0.89}$ . Hence, its hydrogen atoms are better separated from each other, resulting in largely diminished dispersion effects.

The temperature dependences of the  $^1H$  spin-lattice relaxation rates  $R_1$  measured at 23.8 and 90 MHz for  $InPd_3H_{0.89}$  are shown in Fig. 4. The measured proton spin-lattice relaxation rate does not exhibit any pronounced frequency dependence, and its temperature dependence can be described by a linear function,  $R_1(T) = C_e T + R_0$ . Such a behavior is typical of the low-temperature spin-lattice relaxation in metallic hydrides with low concentrations of paramagnetic impurities [30]. The term proportional to the temperature can be identified as the electronic (Korringa) contribution to  $R_1$  resulting from the interaction of proton spins with conduction electrons [30]. The  $R_0$  term can be identified as the low-temperature limit of the paramagnetic contribution to  $R_1$  resulting from the interaction of proton spins with paramagnetic centers. The dashed line in Fig. 4 shows the linear fit to the experimental  $R_1(T)$  data at 90 MHz; the corresponding fit parameters are  $C_e = (2.09 \pm$

$0.04) \times 10^{-3} s^{-1} K^{-1}$  and  $R_0 = 0.02 \pm 0.01 s^{-1}$ . It should be noted that the value of the Korringa constant  $C_e$  (which is proportional to the square of the density of electron states at the Fermi level [30]) for  $InPd_3H_{0.89}$  is considerably lower than that for  $PdH_x$  ( $\sim 1.4 \times 10^{-2} s^{-1} K^{-1}$  for  $x$  in the range 0.70–0.80 [31,32]). In the studied temperature range 28–360 K, we cannot discern any contributions to  $R_1$  resulting from H jump motion. In metal-hydrogen systems, such contributions usually become important when the H jump rate  $\tau^{-1}$  exceeds  $10^6 s^{-1}$ , and leads to a frequency-dependent  $R_1(T)$  peak when  $\tau^{-1}$  becomes nearly equal to the resonance frequency  $\omega$  [30]. Our  $R_1$  results indicate that the value of  $\tau^{-1}$  in  $InPd_3H_{0.89}$  remains below  $10^6 s^{-1}$  at 360 K. This conclusion is supported by the absence of motional narrowing of the  $^1H$  NMR spectrum in  $InPd_3H_{0.89}$ . The measured width of the proton NMR spectrum at half-maximum is found to be nearly constant ( $\sim 17$  kHz) over the temperature range 28–300 K. This value of the line width is consistent with the calculated second moment of the  $^1H$  NMR line for the ‘rigid’ lattice of  $InPd_3H_{0.89}$ ,  $\langle \Delta\omega^2 \rangle = 1.26 \times 10^9 s^{-2}$ . Comparison of our proton NMR results for  $InPd_3H_{0.89}$  with those for Pd hydrides [31,32] shows that H mobility in  $PdH_x$  is much higher. For example, the measured  $R_1(T)$  dependence for  $PdH_{0.7}$  at  $\omega/2\pi = 47$  MHz passes through a maximum close to 270 K [32], which indicates that  $\tau^{-1}$  reaches the value  $3 \times 10^8 s^{-1}$  at this temperature. Such a strong difference between H mobilities in the hydrides with the same type (fcc) of host-metal sublattice can be accounted for in terms of the intersite distances for the hydrogen sublattice. In  $PdH_x$ , hydrogen atoms can occupy all octahedral interstitial sites of the fcc host-metal sublattice, and the distance between the nearest-neighbor octahedral sites is about 285 pm. In  $InPd_3H_{0.89}$ , hydrogen atoms occupy only the octahedral sites with  $[Pd_6]$  coordination, leaving the  $[In_2Pd_4]$  sites empty; the corresponding distance between the nearest-neighbor sites of the H sublattice is 402 pm. Moreover, the nearest-neighbor H sites in  $InPd_3H_{0.89}$  are separated by a Pd atom lying on the line connecting these sites (see Fig. 2). Both the large intersite distances and the blocking effect of Pd atoms are expected to inhibit hydrogen diffusion in  $InPd_3H_{0.89}$ .

Fig. 5 shows the temperature dependence of the  $^2D$  spin-lattice relaxation rate measured at 61.4 MHz for  $InPd_3D_{0.89}$ . As can be seen from the comparison of Figs. 4 and 5 for the isotope-substituted hydrides, the measured relaxation rates for  $^2D$  are much smaller than those for  $^1H$ . This originates mainly from the fact that the gyromagnetic ratio  $\gamma_D$  for  $^2D$  is about 6.5 times

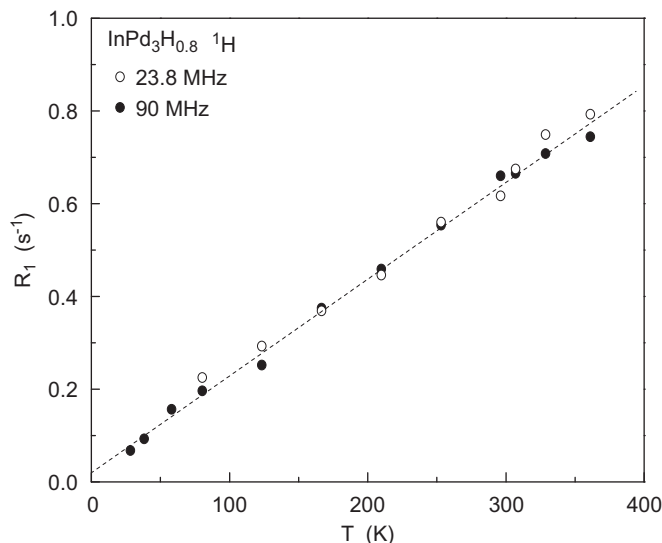


Fig. 4. The temperature dependence of the proton spin-lattice relaxation rates measured at 23.8 and 90 MHz for  $InPd_3H_{0.89}$ . The dashed line shows the linear fit to the data at 90 MHz.

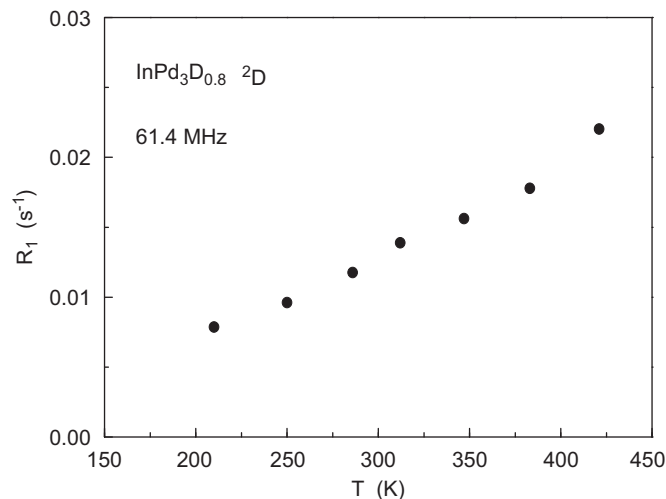


Fig. 5. The temperature dependence of the  $^2D$  spin-lattice relaxation rate measured at 61.4 MHz for  $InPd_3D_{0.89}$ .

smaller than that for  $^1\text{H}$ ,  $\gamma_{\text{H}}$ . The low-temperature limit of the data shown in Fig. 5 is determined mainly by difficulties in measuring very small relaxation rates. As in the case of  $^1\text{H}$  relaxation, the temperature dependence of the  $^2\text{D}$  spin-lattice relaxation rate can be described by a linear function; this suggests that the  $^2\text{D}$  relaxation rate is also dominated by electronic (Korringa) contribution. Assuming that the electronic structure of the deuteride is the same as that of the hydride, we expect that the Korringa contribution to the  $^2\text{D}$  relaxation rate should be a factor of  $(\gamma_{\text{H}}/\gamma_{\text{D}})^2 = 42.4$  smaller than the corresponding contribution to the  $^1\text{H}$  relaxation rate. The ratio of the experimental  $R_1$  values for  $^1\text{H}$  and  $^2\text{D}$  at 310 K is 47.8. The shape of the  $^2\text{D}$  NMR spectrum is close to a Gaussian line, and its width at half-maximum (3.3 kHz) remains unchanged over the studied temperature range 210–421 K. Apart from the absence of motional narrowing, these results suggest the cubic point symmetry of D sites. In fact, since deuterium nuclei have a non-zero electric quadrupole moment, the  $^2\text{D}$  NMR spectrum may exhibit a quadrupole splitting [33] if the symmetry of charge environment of D sites is lower than the cubic one. We have found no signs of quadrupole splitting; this is consistent with the cubic point symmetry of D sites at the centers of the  $[\text{Pd}_6]$  octahedra.

#### 4. Conclusion

Hydrogen introduces an atomic rearrangement from a tetragonal  $\text{ZrAl}_3$  type structure (four-fold ccp superstructure) in  $\text{InPd}_3$  to a cubic  $\text{AuCu}_3$  type structure (one-fold ccp superstructure). Deuterium occupies the octahedral voids defined exclusively by palladium,  $[\text{Pd}_6]$ , to 88.5(6)% in a statistical manner as evidenced by neutron powder diffraction, i.e.,  $\text{InPd}_3\text{D}_{0.89}$  crystallizes in a cubic anti-perovskite type structure. The palladium–deuterium distance of 201.13(1) pm is typical for interstitial hydrides with palladium. Inelastic neutron scattering on the hydride shows a spectrum similar to that of binary palladium hydride but with a sharper and higher-energy peak, which is in accordance with the cubic site symmetry of a  $[\text{Pd}_6]$  interstice. This is also confirmed by the absence of any quadrupole splitting in the  $^2\text{D}$ -NMR signal of the deuteride. The absence of motional narrowing of the  $^1\text{H}$  NMR spectrum in  $\text{InPd}_3\text{H}_{0.89}$  and the relaxation rate  $R_1$  indicate that the value of the H jump rate  $\tau^{-1}$  in  $\text{InPd}_3\text{H}_{0.89}$  remains below  $10^6 \text{ s}^{-1}$  in the studied temperature range 28–360 K. This small hydrogen mobility in  $\text{InPd}_3\text{H}_{0.8}$  as compared to that in the binary palladium hydride, which is orders of magnitude larger, can be attributed to the large spatial separation of  $[\text{Pd}_6]$  sites. Neither INS nor NMR measurements give any hint for a phase transition with ordering of the statistically occupied H(D) positions in  $\text{InPd}_3\text{H(D)}_{0.89}$  as in Laves phase hydrides [34,35].

#### Acknowledgment

This work was supported by the Deutsche Forschungsgemeinschaft (Ko1803/2-1). We thank H. Recktenwald and S. Beetz

(Saarbrücken) for technical assistance, C. Ritter for assistance with the neutron powder diffraction experiments, and J.J. Rush for useful discussions. The Institut Laue-Langevin (Grenoble, France) is gratefully acknowledged for the allocation of beam time.

#### References

- [1] T. Graham, Philos. Trans. R. Soc. London 156 (1866) 399–439.
- [2] T. Graham, Proc. R. Soc. London 17 (1869) 212–220.
- [3] T.B. Flanagan, W.A. Oates, Annu. Rev. Mater. Sci. 21 (1991) 269–304.
- [4] T.B. Flanagan, Y. Sakamoto, Platinum Met. Rev. 37 (1993) 26–37.
- [5] H. Kohlmann, Metal hydrides, in: third ed., in: R.A. Meyers (Ed.), Encyclopedia of Physical Sciences and Technology, vol. 9, Academic Press 2002, pp. 441–458.
- [6] H. Kohlmann, H.E. Fischer, K. Yvon, Inorg. Chem. 40 (2001) 2608–2613.
- [7] H. Kohlmann, Z. Kristallogr. 224 (2009) 454–460.
- [8] K. Baba, Y. Niki, Y. Sakamoto, T.B. Flanagan, A. Craft, Scr. Metall. 21 (1987) 1147–1151.
- [9] H. Kohlmann, G. Renaudin, K. Yvon, C. Wanek, B. Harbrecht, J. Solid State Chem. 178 (2005) 1292–1300.
- [10] N. Kurtzemann, H. Kohlmann, Z. Anorg. Allg. Chem. 636 (2010) 1032–1037.
- [11] H. Kohlmann, J. Solid State Chem. 183 (2010) 367–372.
- [12] H. Kohlmann, C. Ritter, Z. Anorg. Allg. Chem. 635 (2009) 1573–1579.
- [13] J. Rodriguez-Carvajal, FullProf.2k, Version 3.70—Jul2006-ILL JRC, 2006, unpublished.
- [14] T.J. Udovic, C.M. Brown, J. Leão, P.C. Brand, R.D. Jiggetts, R. Zeitoun, T.A. Pierce, I. Peral, J.R.D. Copley, Q. Huang, D.A. Neumann, R.J. Fields, Nucl. Instrum. Methods A 588 (2008) 406–413.
- [15] P. Önnerud, Y. Andersson, R. Tellgren, P. Norblad, F. Bourée, G. André, Solid State Commun. 101 (1997) 433–437.
- [16] K. Yvon, Hydrides: Solid state transition metal complexes, in: R.B. King (Ed.), Encyclopedia of Inorganic Chemistry, vol. 3, Wiley, New York 1994, p. 1401.
- [17] H. Kohlmann, F. Müller, K. Stöwe, A. Zalga, H.P. Beck, Z. Anorg. Allg. Chem. 635 (2009) 1407–1411.
- [18] R.V. Denys, A.B. Riabov, V.A. Yartys, B.C. Hauback, H.W. Brinks, J. Alloys Compd. 356–357 (2003) 65–68.
- [19] M. Wendorff, H. Scherer, C. Röhr, Z. Anorg. Allg. Chem. 636 (2010) 1038–1044.
- [20] V.A. Somenkov, A.V. Irodova, J. Less-Common Met. 101 (1984) 481–492.
- [21] A.V. Skripov, J.C. Cook, T.J. Udovic, V.N. Kozhanov, R. Hempelmann, Appl. Phys. A: Mater. Sci. Process. 74 (Suppl.) (2002) S948–S950.
- [22] H. Kohlmann, N. Kurtzemann, R. Wehrich, T. Hansen, Z. Anorg. Allg. Chem. 635 (2009) 2399–2405.
- [23] D. Richter, R. Hempelmann, R.C. Bowman, in: L. Schlapbach (Ed.), Hydrogen in Intermetallic Compounds, vol. II, Springer, Berlin 1992, p. 97.
- [24] D.K. Ross, in: H. Wipf (Ed.), Hydrogen in Metals, vol. III, Springer, Berlin 1997, p. 153.
- [25] T.J. Udovic, J.J. Rush, I.S. Anderson, R.G. Barnes, Phys. Rev. B 41 (1990) 3460–3465.
- [26] B. Hauer, R. Hempelmann, T.J. Udovic, J.J. Rush, E. Jansen, W. Kockelmann, W. Schäfer, D. Richter, Phys. Rev. B 57 (1998) 11115–11124.
- [27] D.K. Ross, V.E. Antonov, E.L. Bokhenkov, A.I. Kolesnikov, E.G. Ponyatovsky, J. Tomkinson, Phys. Rev. B: Condens. Matter Mater. Phys. 58 (1998) 2591–2595.
- [28] M. Kemali, J.E. Totolici, D.K. Ross, I. Morrison, Phys. Rev. Lett. 84 (2000) 1531–1534.
- [29] J.M. Rowe, J.J. Rush, H.G. Smith, M. Mostoller, H.E. Flotow, Phys. Rev. Lett. 33 (1974) 1297–1300.
- [30] R.G. Barnes, in: H. Wipf (Ed.), Hydrogen in Metals, vol. III, Springer, Berlin 1997, p. 93.
- [31] G.K. Schoep, N.J. Poulis, R.R. Arons, Physica 75 (1974) 297–304.
- [32] D.A. Cornell, E.F.W. Seymour, J. Less-Common Met. 39 (1975) 43–54.
- [33] A. Abragam, in: The Principles of Nuclear Magnetism, Clarendon Press, Oxford, 1961.
- [34] H. Kohlmann, K. Yvon, J. Alloys Compd. 309 (2000) 123–126.
- [35] H. Kohlmann, F. Fauth, P. Fischer, A.V. Skripov, K. Yvon, J. Alloys Compd. 327 (2001) L4–L9.